New Journal of Physics
The open-access journal for physics

Resonant ratcheting of a Bose–Einstein condensate

L Morales-Molina[1] **and S Flach**[2]

[1] Department of Physics, National University of Singapore, 117542, Republic of Singapore
[2] Max-Planck-Institut für Physik Komplexer Systeme, Nöthnitzer Strasse 38, 01187 Dresden, Germany

New Journal of Physics **10** (2008) 013008 (13pp)
Received 4 October 2007
Published 14 January 2008
Online at http://www.njp.org/
doi:10.1088/1367-2630/10/1/013008

Abstract. We study the rectification process of interacting quantum particles in a periodic potential exposed to the action of an external ac driving. The breaking of spatio-temporal symmetries leads to directed motion even in the absence of interactions. A hallmark of quantum ratcheting is the appearance of resonant enhancement of the current (Denisov *et al* 2007 *Europhys. Lett.* **79** 10007; Denisov *et al* 2007 *Phys. Rev.* A **75** 063424). Here, we study the fate of these resonances within a Gross–Pitaevskii equation which describes a mean field interaction between many particles. We find that the resonance (i) is not destroyed by interactions, (ii) shifts its location with increasing interaction strength. We trace the Floquet states of the linear equations into the nonlinear domain, and show that the resonance gives rise to an instability and thus to the appearance of new nonlinear Floquet states, whose transport properties differ strongly as compared to the case of noninteracting particles.

Contents

1. Introduction

The breaking of space-time symmetries, and its role in the generation of directed transport in single particle Hamiltonian ratchets, has been extensively studied in the classical [1]–[3] and quantum regimes [4]–[8]. Experiments with thermal cold atoms loaded on optical lattices [9] demonstrated the fruitfulness and correctness of the theoretical predictions. Importantly, the latest studies show a resonant enhancement of the current in the quantum regime, due to resonances between Floquet states [5, 6]. Real experiments involve many atoms, and interaction between them may be tuned, but will always be left at least at some residual nonzero level. Therefore, the impact of interactions on quantum ratchets has to be addressed. As recently shown by Poletti *et al* [10] for a kicked system, interaction may lift accidental symmetries of the single particle dynamics and change the current values.

In this paper, we study, using the mean-field approach, the generation of directed transport of interacting quantum particles in a periodic potential under the action of a two harmonic driving. With this approach we mimic the motion of cold atoms in an optical lattice in the presence of an external force [9], but at much lower temperatures, when a Bose–Einstein condensate may form [11]. To this end, we investigate the continuation of Floquet states of the corresponding linear system into the nonlinear domain. We show that a resonant enhancement of the current in the nonlinear regime takes place, which results from the resonant interaction between *nonlinear Floquet states*. We derive an analytical expression for the evolution of quasienergies in the nonlinear regime. Finally we show the relation between the transport properties of nonlinear Floquet states and the asymptotic current of an initial state with zero momentum.

2. Model

Experimental realizations of ratchets with cold atoms may tune the temperatures from milliKelvin down to microKelvin, such that a Bose–Einstein condensate may form due to interactions between particles [11]. The corresponding general equation to be studied is then given by the one-dimensional Gross–Pitaevskii equation (see e.g. [12])

$$\mathrm{i}\hbar\frac{\partial\Psi(\tau)}{\partial\tau}=\left[-\frac{\hbar^2}{2M}\frac{\partial^2}{\partial X^2}+V_0\cos(2k_{\mathrm{L}}X)-Xe(\tau)\right]\Psi+\frac{4\pi\hbar^2a_{\mathrm{s}}}{M}|\Psi|^2\Psi, \tag{1}$$

where a_{s} is the s-wave scattering length, M is the atomic mass, $k_{\mathrm{L}}=\pi/d$ is the optical lattice wave number with optical step d, V_0 is the periodic potential depth, and $e(\tau)$ is a periodic driving force. The wavefunction is normalized to the total number of atoms in the condensate and we define n_0 as the average uniform atomic density [12, 13].

Introducing the dimensionless variables $x=2k_{\mathrm{L}}X$, $t=\tau/t_{\mathrm{s}}$, $\psi=\Psi/\sqrt{n_0}$, and defining $1/\mu=M/4\hbar k_{\mathrm{L}}^2t_{\mathrm{s}}$; we transform the system (1) to the dimensionless equation [10]

$$\mathrm{i}\mu\frac{\partial\psi(t)}{\partial t}=H_0\psi+g|\psi|^2\psi, \tag{2}$$

where the dimensionless one-particle Hamiltonian is

$$H_0=\tfrac{1}{2}\hat{p}^2+v_0\cos(x)-xE(t), \tag{3}$$

with $\hat{p}=-\mathrm{i}\mu\frac{\partial}{\partial x}$ and rescaled parameters $v_0=\mu^2MV_0/4\hbar^2k_{\mathrm{L}}^2=1$, $E(t)=\mu^2Me(t)/8\hbar^2k_{\mathrm{L}}^3$ and $g=\mu^2C$ with $C=\pi n_0a_{\mathrm{s}}/k_{\mathrm{L}}^2$ [12]. The dimensionless ac field $E(t+T)=E(t)$.

As in the linear limit [5, 6], we consider $E(t) = E_1 \cos[\omega(t - t_0)] + E_2 \cos[2\omega(t - t_0) + \theta]$ with t_0 as initial time.

By using the gauge transformation, $|\psi\rangle \to \exp[\frac{\mathrm{i}}{\mu} x A(t)]|\psi\rangle$, where $A(t) = -E_1 \sin[\omega(t - t_0)]/\omega - E_2 \sin[2\omega(t - t_0) + \theta]/2\omega$ is the vector potential [5, 6]; we transform the original one-particle Hamiltonian to

$$H_0 = \tfrac{1}{2}[\hat{p} - A(t)]^2 + \cos(x). \tag{4}$$

2.1. Linear regime

Consider the Schrödinger equation, the linear limit of equations (2)–(4). Here, we use a tilde to denote wavefunctions, quasienergies and other relevant parameters for the linear regime.

It was shown in [5, 6] that, for the appearance of a dc-current in the quantum regime, two symmetries need to be broken. These symmetries are defined in the classical limit as follows [1]. If $E(t)$ is shift symmetric $E(t) = -E(t + T/2)$, then the Hamiltonian (3) is invariant under the transformation

$$S_\mathrm{a} : (x, p, t) \to (-x, -p, t + T/2). \tag{5}$$

Likewise if $E(t)$ possesses the symmetry $E(t) = E(-t)$, then (3) is invariant under the transformation

$$S_\mathrm{b} : (x, p, t) \to (x, -p, -t). \tag{6}$$

The Hamiltonian equation (3) is a periodic function of time. Then the solutions, $|\tilde{\psi}(t + t_0)\rangle = U(t, t_0)|\tilde{\psi}(t_0)\rangle$, can be characterized by the dynamics of the eigenfunctions of $U(T, t_0)$ which satisfy the Floquet theorem:

$$|\tilde{\psi}_\alpha(t)\rangle = \mathrm{e}^{-\mathrm{i}(\tilde{\epsilon}_\alpha/T)t}|\tilde{\phi}_\alpha(t)\rangle, \qquad |\tilde{\phi}_\alpha(t + T)\rangle = |\tilde{\phi}_\alpha(t)\rangle. \tag{7}$$

The quasienergies $\tilde{\epsilon}_\alpha(-\pi < \tilde{\epsilon}_\alpha < \pi)$ and the Floquet eigenstates can be obtained as solutions of the eigenvalue problem of the Floquet operator

$$\tilde{U}(T, t_0)|\tilde{\psi}_\alpha(t_0)\rangle = \mathrm{e}^{-\mathrm{i}\tilde{\epsilon}_\alpha}|\tilde{\psi}_\alpha(t_0)\rangle. \tag{8}$$

Due to the discrete translational invariance of equation (4) and Bloch's theorem all Floquet states are characterized by a quasimomentum κ with $|\tilde{\psi}_\alpha(x + 2\pi)\rangle = \mathrm{e}^{\mathrm{i}\hbar\kappa}|\tilde{\psi}_\alpha(x)\rangle$.

We choose $\kappa = 0$ which corresponds to initial states where atoms equally populate all (or many) wells of the spatial potential. This allows us to use periodic boundary conditions for equation (2), with spatial period $L = 2\pi$, so that the wave function can be expanded in the plane wave eigenbasis of the momentum operator $\hat{p}$, $|n\rangle = \frac{1}{\sqrt{2\pi}}\mathrm{e}^{\mathrm{i}nx}$, viz

$$|\tilde{\psi}(t)\rangle = \sum_{n=-N}^{N} c_n(t)|n\rangle. \tag{9}$$

Thus, the Floquet operator is obtained by solving equations (2)–(4) in the linear limit. In the computations we neglect the contribution originating from $A(t)^2$, since it only yields a global phase factor. Details of the numerical method are given in [6]. A study of a related problem with nonzero κ has been published in [4], which shows that the essential features of avoided crossings survive. Once the Floquet evolution operator is computed, one finds that the symmetries of the classical equations of motion are reflected by corresponding symmetries of the Floquet operator. If the Hamiltonian is invariant under the shift symmetry S_a (5), then

the Floquet operator possesses the property $U(T,t_0)=U^{\Pi T}(T/2,t_0)U(T/2,t_0)$ [5, 6]. Here U^{Π} performs a transposition along the codiagonal of U. With our driving function $E(t)$, S_a is always violated. If the Hamiltonian is invariant under the time reversal symmetry S_b (6), then the Floquet operator has the property $U(T,t_0)=U(T,t_0)^{\Pi}$ [5, 6, 14].

To estimate the net transport, it is necessary to compute the asymptotic current. It is obtained using the expression $J(t_0)=\sum_\alpha \langle p\rangle_\alpha |C_\alpha(t_0)|^2$ [6], where $\langle p\rangle_\alpha$ are the Floquet states momenta and $C_\alpha(t_0)$ are the expansion coefficients of the initial wave function in the basis of Floquet states. Breaking the symmetries S_a (5) and S_b (6), we desymmetrize the Floquet states, i.e. the Floquet states momenta acquire a finite value $\langle p\rangle_\alpha \neq 0$, which results in the appearance of a directed transport.

In general, the current is a function of the initial time t_0 and the relative phase θ, namely $J(t_0,\theta)$. After averaging over the initial time it exhibits the property [5, 6]:

$$J(\theta)=-J(\theta+\pi)=-J(-\theta). \tag{10}$$

We focus the analysis on previous computations obtained for $\mu=0.2$ in [5, 6].

Figure 1(a) shows a section of the quasienergy spectrum of the Floquet states versus θ for the interval $[-\pi,0]$, where a resonance of states, i.e. an avoided crossing, takes place. The quasienergies of the system equations (2)–(4) in the linear limit possess the property [5, 6]

$$\tilde{\epsilon}_\alpha(\theta)=\tilde{\epsilon}_\alpha(-\theta). \tag{11}$$

Figure 1(b) shows the current dependence on θ. The computation is performed taking the initial state $|0\rangle=1/\sqrt{2\pi}$, which overlaps with states in the chaotic layer. With this initial condition we mimic a dilute gas of atoms which are spread all over the lattice with zero momentum. The current has two peaks which are linked to avoided crossings displayed in figure 1(a). In these particular avoided crossings, states from the chaotic layer and transporting states mix, which leads to a leakage from the chaotic layer to the transporting state, thereby enhancing the current.

On the other hand, it was shown in [5, 6] that by tuning the amplitude of the second harmonic of the driving force the peaks becomes broader which makes it easier resolving it in experiments (see dashed line in figure 1(b)).

2.2. Nonlinear regime

In the nonlinear case the analysis of the generation of directed transport in the presence of a driving force is much more complicated, due to possible nonintegrability, classical chaos, and mixing [15]. However, one can take the Floquet states of the linear problem, and continue them as periodic orbits into the nonlinear regime. Then these nonlinear Floquet states can be analyzed.

While in the linear regime the evolution of the Floquet state is determined by equation (8) with a unitary operator U, in the nonlinear regime the unitarity is lost, and is replaced locally by simplectic maps [16]. Nevertheless, a similar transformation over one period of the ac driving can be defined, viz

$$U\psi_\alpha(0)=\exp(-\mathrm{i}\epsilon_\alpha)\psi_\alpha(0), \tag{12}$$

where U is a nonlinear map of the phase space on to itself, defined by integrating a given trajectory over one period of the ac driving [17]. The solutions ψ_α constitute generalizations of the linear Floquet states (7).

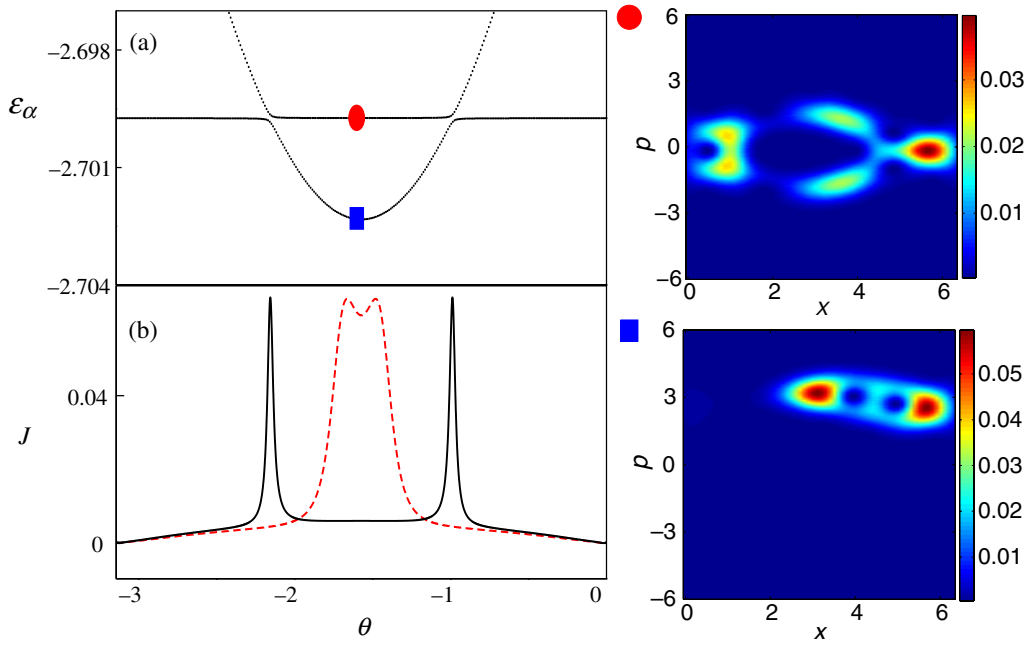

Figure 1. Left panel: (a) two bands of quasienergies in the linear regime whose interaction leads to avoided crossings. Symbols placed in different bands correspond to states with Husimi functions depicted in the right panel. Here $E_2 = 1.2$. (b) Average current J versus θ for different amplitude values of the second harmonic E_2: 1 (dashed line) and 1.2 (solid line). Right panel: Husimi functions of two different Floquet states labeled by a circle and square for $t_0 = 0$. We use the Husimi function defined in [6]. Bands and current are plotted for the interval $(-\pi, 0)$. Here the quasienergies are symmetric with respect to a reflection in θ as deduced from equation (11), while from equation (10) it follows that the current is antisymmetric with respect to a reflection at the origin. The other parameters are $E_1 = 3.26$ and $\omega = 3$.

To compute the nonlinear Floquet states, we use a numerical method implemented in computational studies of periodic orbits [17]. The basics steps are as follows. First, we choose a linear Floquet state as an initial seed. Then taking a small value of the nonlinearity strength, we compute the new solution using a Newton–Raphson iterative procedure, by varying initial seed (see appendix A for a detailed explanation). The procedure involves conservation of the norm and the variation of the quasienergy of the state, which together enforce the convergence to the desired solution. In each iteration step, the new trial solution is integrated over one time period T. Once a solution is found, we increase the nonlinearity strength again by a small amount and repeat the same procedure. Thus, we trace the solution into the nonlinear domain.

Desymmetrization of the Floquet states, due to breaking of symmetries, leads to the appearance of directed transport in the linear regime with enhancement of transport due to resonant Floquet states. It is therefore worthwhile to investigate what happens with nonlinear Floquet states in the absence of those symmetries, and trace the fate of the abovementioned resonances in the nonlinear regime.

2.2.1. Dimer. To gain insight into the effect of breaking symmetries on nonlinear Floquet states, we utilize a basic model of two coupled BEC states in the presence of an external driving. The equations for a driven two sites model can be written as

$$\mathrm{i}\mu\frac{\mathrm{d}\psi_1}{\mathrm{d}t} = C\psi_2 + g\,\psi_1 N_1 + \mu\psi_1 f(t), \tag{13}$$

$$\mathrm{i}\mu\frac{\mathrm{d}\psi_2}{\mathrm{d}t} = C\psi_1 + g\,\psi_2 N_2 - \mu\psi_2 f(t), \tag{14}$$

where $f(t) = f_1\sin(\omega t) + f_2\sin(2\omega t + \theta)$, C is the coupling term, and $N_{1,2} = |\psi_{1,2}|^2$ are the populations or number of particles in the sites 1 and 2. The above equations can be also qualitatively viewed as a restriction of the original case (4) to just two basis states with opposite momenta. That leads to the corresponding different signs of the last terms in the rhs of the above equations.

With $f(t) = 0$ the equations above are used to describe, on the mean field level, the self-trapping transition of two coupled BEC. It was shown in [18, 19] that such a phenomenon occurs when the nonlinearity exceeds a critical value, and the new states are characterized by a population imbalance N_1–N_2. The existence of critical or threshold values have been predicted as well [18]. The critical value is determined by the bifurcation point of the stationary solutions. The selftrapped states violate the permutational symmetry of (13) and (14), which implies that the equations are invariant under permutation of the two indices. If $f(t) \neq 0$, the permutational symmetry is broken in general. If however $f(t)$ is antisymmetric, then the dimer equations are invariant under the combined action of permutation *and* time reversal.

Let us consider the linear case $g = 0$ first. For $f(t) = 0$ the stationary solutions are the in- and out-of-phase modes $\psi_1(t) = \pm\psi_2(t) = (1/\sqrt{2})\mathrm{e}^{\mp\mathrm{i}(C/\mu)t}$, which are in fact strictly time-periodic states, with period $2\pi\mu/C$. Adding the ac drive $f(t)$ they transform into two linear Floquet states. They will start to become asymmetric, since the presence of $f(t)$ violates permutational invariance, *but only if $f(t)$ is also violating time-reversal antisymmetry*. Note that if $f(t)$ is antisymmetric, the original ac field $E(t)$ is symmetric. If on the contrary time-reversal antisymmetry is in place, the linear Floquet states will still be invariant under the combined action of permutation, time reversal and complex conjugation. Thus they do not acquire any population imbalance. Also the Floquet states will now acquire a nonzero phase shift $e^{-\mathrm{i}\nu T}$, where $\nu \approx \frac{C}{\mu}$ in the limit $f(t) \to 0$, when iterated over one period of the driving T.

In the presence of nonlinearity close to these linear Floquet states there will be again states, which are 'periodic' in the sense that after one period of the ac driving the state returns to itself, up to a corresponding phase. Note that both the shape of the eigenstate, but also the phase (i.e. the analogue of the quasienergy in the linear case) will smoothly change upon continuation into the nonlinear regime. The continuation process of such a nonlinear Floquet state is thus encoded by the linear Floquet state at $g = 0$, which is chosen to be continued.

In the case of f_1, f_2 being nonzero, θ becomes a relevant parameter. For $\theta \neq 0, \pi$ time-reversal antisymmetry is broken, and the nonlinear Floquet solutions will also loose that symmetry, together with the permutational symmetry (see above).

Hereafter, we name by symmetric the case when $\theta = 0, \pi$ and nonsymmetric otherwise. We will also coin linear and nonlinear Floquet states *periodic orbits*, although they are only periodic up to the above mentioned phase shift.

Figure 2 shows the result of continuation of one periodic orbit for the symmetric and non-symmetric driven dimer, which corresponds to the symmetric eigenstate of the linear undriven

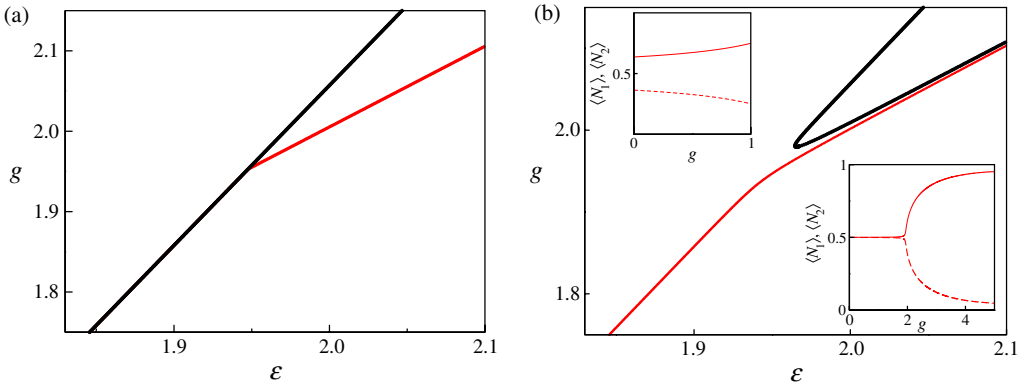

Figure 2. Nonlinearity parameter g versus quasienergies for one of the nonlinear Floquet states. (a) $\theta = 0$. (b) $\theta = -1.6$. Bottom-right inset shows the average populations over a period T as a function of the nonlinearity strength g. Top-left inset is the enlargement around $g = 0$ of the bottom-right inset. The parameters are $\omega = 2\pi$, $f_1 = f_2 = 1$, $C = 1$ and $\mu = 1$.

system. The symmetric case shows a pitchfork bifurcation with the appearance of two new states at the bifurcation point (figure 2(a)). These new states exhibit a population imbalance similar to the undriven system [18], [20]–[22], despite the fact that the equations are symmetric.

This bifurcation is a hallmark of the presence of nonlinearity. Out of a given Floquet state several new states are emerging, while for the linear case the number of linear Floquet states is fixed by the size of the chosen basis.

Conversely, if the time-reversal symmetry is broken, a saddle-node bifurcation appears. First of all the state continued from the linear limit, already acquires some nonzero population imbalance, since the symmetry is broken. Figure 2 shows that the strict continuation of that state evolves into a state with a strong population imbalance. Two other states—one which is corresponding to a weak imbalance, and another which has a strong imbalance as well—emerge through the saddle-node bifurcation.

To conclude this part, we may expect that nonlinearity induces Floquet states with nonzero population imbalance via bifurcations, or enhances the already present imbalance (originating from a symmetry breaking) again via bifurcations. We remind the reader here, that the simple dimer model can be obtained from (4) by choosing two momentum basis states with different sign, and replacing the original complicated interaction which is mediated via further basis states, by a direct interaction term. A population imbalance thus means a momentum imbalance as well, i.e. a nonzero current. It may be thus as well expected, that for the full problem, to be treated below, nonlinearity may enhance directed currents via bifurcations.

2.2.2. Full lattice. The analysis of nonlinear Floquet states in the dimer suggests the formation of states with nonzero mean momentum above a certain threshold value. The question then arises, to what extent those features, exhibited by the Floquet states in the dimer, are manifested in the full lattice equations (2)–(4).

On the other side, the question about the fate of the resonances found in the linear limit remains. It is therefore of particular interest to analyse those resonant Floquet states, which lead to an enhancement of transport in the linear regime. By switching on the nonlinearity in

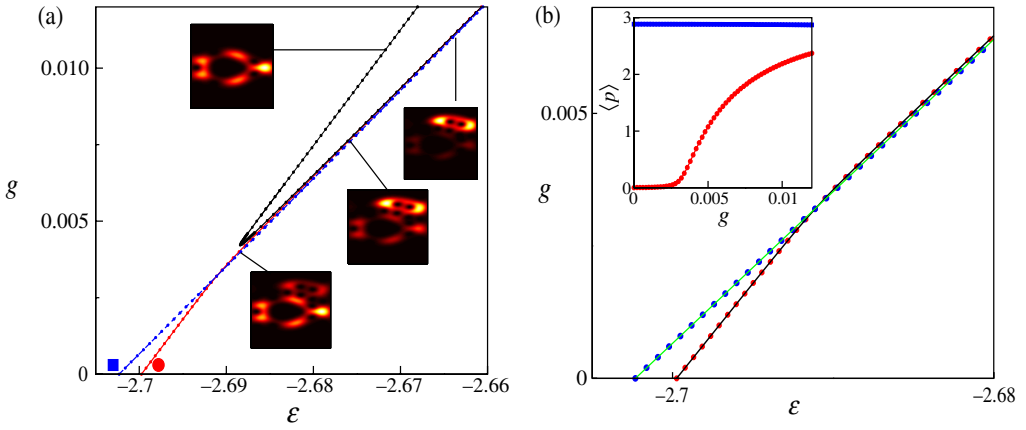

Figure 3. (a) Nonlinearity strength versus quasienergy of periodic solutions. The periodic solutions are a continuation from the Floquet states displayed in figure 1. The symbols link to states displayed in figure 1. Insets: Husimi functions (P vs X) (cf figure 1). The sequence of Husimi functions for the red line is explained in the text. (b) Enlargement of the region where the quasienergies of the continued original states intersect in panel (a). The results from the computation of equation (16) appear superimposed to the circles with solid lines. Inset: mean average momentum of periodic solutions versus nonlinearity strength. Blue square: momentum of the state depicted by a blue circles-dashed line in (a). Red circle: momentum of the state depicted by a red circles-dashed line in (a). The parameters are $E_1 = 3.26$, $E_1 = 1.2$, $\theta = -1.6$ and $\omega = 3$.

equation (2), the system in the linear regime gets perturbed and the resonances are shifted to different values of the control parameters.

In figure 3, we present the continuations of two Floquet states depicted in figure 1, into the nonlinear domain. We observe a bifurcation of one of the periodic states as we increase the nonlinearity strength. Here, as in the dimer, a bifurcation of saddle-node type leads to the formation of three periodic solutions out of one.

Since we want to study the transport of a BEC with zero initial momentum, we focus on the continuation of the state lying in the chaotic layer. The continuation process is indicated by a sequence of Husimi functions in figure 3(a), and can be summarized as follows: (i) before the bifurcation, the state is located in the chaotic layer; (ii) after the bifurcation, the periodic state transforms into a mixed state due to a resonance with a second transporting state; (iii) further increase of the nonlinearity strength transforms it into a transporting state. By contrast, the originally transporting state does not experience significant changes as we increase the nonlinearity strength.

A quantitative measure of this transition process is given by the evolution of the average momentum of the periodic states as we change the nonlinearity strength (figure 3(b)). The momentum of the state initially located in the chaotic layer goes from small to high values with a sharp increase at $g \approx 0.003$ (i.e. at the bifurcation point), whereas the momentum for the transporting state remains nearly a constant.

So far, we have analyzed the evolution of two states in the nonlinear domain. A clear message from the above results is, that nonlinear Floquet states may drastically change their

average momentum at bifurcations, which are also visible through sharp changes in the dependence of their quasienergies on the nonlinearity parameter.

In order to estimate the shift of the bifurcation point, and to finally predict the new possible resonance positions with increasing nonlinearity, we use a perturbation approach to estimate the dependence $\epsilon = P(\tilde{\epsilon}, g)$, related to the Aharanov–Anandan phase [23] (see also [16]). Assume that nonlinear periodic solutions and Floquet states are related through a dynamical phase $\lambda(t)$, i.e. $\phi(t) = \exp[-\mathrm{i}\lambda(t)]\tilde{\phi}(t)$ with $\lambda(T) - \lambda(0) = 2k\pi$, $k = 0, \pm 1, \pm 2, \ldots$.

Then for $k = 0$ we find (see appendix B for details)

$$\epsilon(\theta, g) = \tilde{\epsilon}(\theta) + \frac{g}{\mu}\int_0^T \mathrm{d}t\,\langle\phi||\phi|^2|\phi\rangle, \tag{15}$$

where $\langle\cdots\rangle = \int_0^{2\pi}\ldots\,\mathrm{d}x$ is the inner product defined in the Hilbert space of Floquet states. From equation (15) it follows that states with strong nonlinear interaction have large quasienergy variations. This allows to resonantly couple states located deep in the well, which exhibit strong localization, with other states. These resonant couplings are beyond the dimer model discussed above.

Bifurcations of new states correspond to a coalescence of different families of states, leading to $\phi_j(t) = \exp[-\mathrm{i}\lambda_j(t)](a_j\tilde{\phi}_1(t) + b_j\tilde{\phi}_2(t))$, where $\tilde{\phi}_1(t)$ and $\tilde{\phi}_2(t)$ are the corresponding original Floquet states. The evolution of the quasienergies for the nonlinear periodic states is thus given by

$$\epsilon_j(\theta, g) = |a_j|^2\tilde{\epsilon}_1(\theta) + |b_j|^2\tilde{\epsilon}_2(\theta) + \frac{g}{\mu}\int_0^T \mathrm{d}t\,\langle\phi_j||\phi_j|^2|\phi_j\rangle, \tag{16}$$

where a_j and b_j are the corresponding weightings of the linear states in the nonlinear state expansion (see appendix B for details).

In figure 3(b), we plot the quasienergy values computed with equation (16), using the nonlinear states continued from the original linear states depicted in figure 1. We find an excellent agreement with the full numerical results.

For weak nonlinearity, the quasienergies of the states depend linearly on g. A simple perturbation expansion allows us to take the wavefunctions of the original linear states and its respective quasienergies with equation (15). Then from the quasienergy intersection of the two states, $\epsilon_1(\theta, g) = \epsilon_2(\theta, g)$, we compute the critical value of g:

$$g = \frac{\mu[\tilde{\epsilon}_2(\theta) - \tilde{\epsilon}_1(\theta)]}{\int_0^T\int_0^{2\pi}|\tilde{\phi}_1|^4\,\mathrm{d}x\,\mathrm{d}t - \int_0^T\int_0^{2\pi}|\tilde{\phi}_2|^4\,\mathrm{d}x\,\mathrm{d}t}. \tag{17}$$

Inserting the wave function of the original linear states depicted in figure 1 in equation (17), we obtain $g = 0.003008$, which is a good estimate of the nonlinearity strength at the bifurcation point. Let us now investigate the evolution of the state $|0\rangle$ for $\kappa = 0$. In the linear regime, we use the Floquet representation to derive the expression for the asymptotic current. In the nonlinear regime it is no longer possible. Instead, we compute the running average momentum $P = \frac{1}{(t-t_0)}\int_{t_0}^{t}\bar{p}\,\mathrm{d}t$ with $\bar{p} = \langle\psi|\hat{p}|\psi\rangle$, over long times, which becomes the asymptotic current in the limit $t \to \infty$, i.e. $J(t_0) = \lim_{t\to\infty} P$. To validate the convergence to the asymptotic current we use maximum integration times ranging from 100 000 to 300 000 time periods.

First we compute the current for $\theta \approx -0.99$. In such a case, for $g = 0$, there is an avoided crossing (see above discussion), i.e. a resonance. Further increase of the nonlinearity leads to a decay of the current (figure 4). However, taking $\theta = -1.1, -1.2$, we observe a corresponding

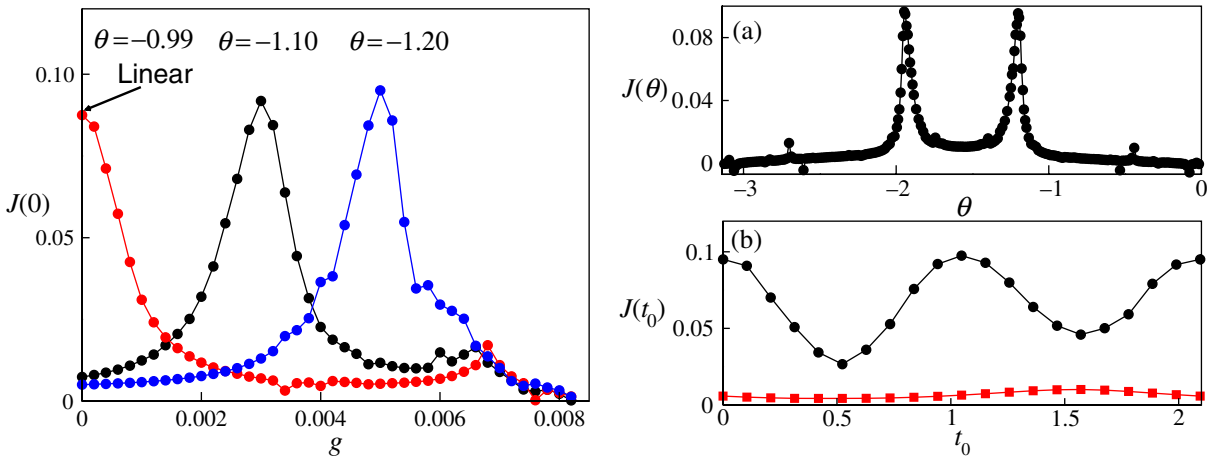

Figure 4. Left panel: current dependence upon the nonlinearity strength g for $\theta = -1.2, -1.1, -0.99$ with initial time $t_0 = 0$. Right panel: (a) current dependence upon θ for g=0.005 with $t_0 = 0$. (b) Current as a function of the initial time for $\theta = -1.2$ and two different nonlinearity strengths. Circles: $g = 0.005$ and squares: $g = 0.001$. The other parameters are $E_1 = 3.26$, $E_1 = 1.2$ and $\omega = 3$.

shift of the resonance peak to larger values of the nonlinearity parameter, thus showing a robustness of the resonant current enhancement observed in the linear limit.

Figure 4 shows the dependence of the current on θ. Resonances similar to the linear case are observed, which are shifted in θ. Thus the nonlinearity strength can also be used as a control parameter for tuning resonances.

It was shown for the linear regime [5, 6] that the current depends upon the initial time t_0. In the nonlinear case, the dynamics may exhibit similar behavior to classical chaos [15], making the analysis more complicated. An essential point here is that, while in the linear regime Floquet states mix in narrow parameter regions via avoided crossings, in the nonlinear domain mixed states may survive for a fairly large range of nonlinearity values. This, along with the fact of having multiple bifurcations with the appearance of new periodic states [24], may lead to classical-like chaotic behavior predicted in [15].

A benchmark for the persistence of directed transport is that the sum of currents for different initial times do not cancel. To check this, we compute the momentum evolution for different initial times with the system in and out of resonance. In figure 4, we present the current dependence upon the initial time t_0. The curve depicted by filled circles shows a similar behavior to the one obtained in the linear regime with the system in resonance (cf figure 4 in [5]). It also displays a large positive current for all initial times, thus confirming the existence of directed motion. On the contrary, the curve with squares shows a nearly flat profile with smaller current values, recalling the off resonance scenario in the linear limit.

3. Conclusions

We have studied the rectification of interacting quantum particles in a periodic potential exposed to the action of an external ac driving, using a mean-field approach.

We showed that by tuning the nonlinearity in an optical lattice it is possible to enhance the directed transport of cold atoms. A possible experimental way to achieve it is to vary the

scattering length by changing the strength of the magnetic field [25]. These resonances are partly continued from the noninteracting system, but become saddle node bifurcations of more complicated nonlinear Floquet states in the nonlinear system under consideration.

We developed analytical estimates of the nonlinearity strength in the resonance, and showed that the evolution of an initial state with zero momentum carries all the signatures of a ratchet state, i.e. its average momentum is nonzero. Therefore, ratchets and quantum resonances of (nonlinear) Floquet states are robust with respect to interactions, and should be observable in real experiments. It is possible that such resonances may even lead to a partial depletion of the condensate fraction, and evaporation. Another issue is the loss of coherence due to incoherent transitions to excited states. In this case, a more suitable description is given by using a master-like equation with dissipation [26].

Finally, bifurcations of the nonlinear Floquet states have been observed, which may affect the measured currents strongly.

Appendix A. Numerical procedure for the computation of nonlinear Floquet states

Take equation (12)

$$U\psi_\alpha(0) = \exp(-\mathrm{i}\epsilon_\alpha)\psi_\alpha(0), \tag{A.1}$$

where ψ_α are periodic solutions in the nonlinear domain and U is a symplectic operator. The periodic states $\psi_\alpha(0)$ are decomposed into real and imaginary parts as $\vec{\Phi}_\alpha = \{\mathrm{Real}[\psi_\alpha(0)], \mathrm{Im}[\psi_\alpha(0)]\}$. Likewise, we define the vector $\vec{\Omega} = \{\mathrm{Real}[\exp(\mathrm{i}\epsilon_\alpha)U\psi_\alpha(0)], \mathrm{Im}[\exp(\mathrm{i}\epsilon_\alpha)U\psi_\alpha(0)]\}$. For convenience we write them as $2N$ dimensional vectors $\vec{X}_\alpha(0) = \vec{\Phi}_\alpha(0)$ and $\vec{X}_\alpha = \vec{\Omega}[\Phi_\alpha(0)]$, where N is the dimension of the Hilbert space [27]. Hereafter, for simplicity, we drop the index α.

The two vectors $\vec{X}$ and $\vec{X}(0)$ are identical for the linear case. Assuming weak nonlinearity, we compute the vector $\vec{X}$ after one integration period, taking as initial seed the linear state $\vec{X}(0)$. This implies that after a full integration period our final state deviates from the initial state:

$$\vec{G}[\vec{X}(0)] = \vec{X} - \vec{X}(0). \tag{A.2}$$

To correct such a deviation we use the Newton–Raphson method. Basically, the method updates the initial seed $\vec{X}(0)$ after every iteration until each component of $\vec{G}$ is reduced to a value less than 10^{-9}. For every integration over the period T, we use the split operator method.

To successfully accomplish the reduction of the vector difference (A.2), some constraints should be fulfilled. First, the Floquet states should preserve the norm. We thus add another component $G_{2N+1} = \vec{X}\vec{X} - \vec{X}(0)\vec{X}(0)$, and the iteration process is also zeroing this component.

To fully characterize our nonlinear Floquet states, we define the new variable vector $\vec{Y} = (\vec{X}, \epsilon)$, with the quasienergy as the $2N+1$ component. Next, we define the new vector function $\vec{F}(\vec{Y}) = [\vec{G}(\vec{Y}), G_{2N+1}(\vec{Y})]$. Having $2N+1$ variables and $2N+1$ functions to be zeroed, we now may apply standard Newton–Raphson methods.

Appendix B. Quasienergy dependence on the nonlinearity strength

We define an expression similar to equation (7), but for the nonlinear case, viz

$$|\psi(t)\rangle = \mathrm{e}^{-\mathrm{i}(\epsilon/T)t}|\phi(t)\rangle, \qquad |\phi(t+T)\rangle = |\phi(t)\rangle. \tag{B.1}$$

Here, we have dropped the index α.

Then, inserting equation (B.1) into equation (2), one finds

$$\mathrm{i}\mu\frac{\partial}{\partial t}|\phi\rangle = \mathcal{H}|\phi\rangle, \tag{B.2}$$

where $\mathcal{H} = H_0 - \frac{\mu}{T}\epsilon + g|\phi|^2$. Similarly, using equation (7) we get for the linear case

$$\mathrm{i}\mu\frac{\partial}{\partial t}|\tilde{\phi}\rangle = \tilde{\mathcal{H}}|\tilde{\phi}\rangle, \tag{B.3}$$

where $\tilde{\mathcal{H}} = H_0 - \frac{\mu}{T}\tilde{\epsilon}$.

Now define $\phi(t) = \exp[-\mathrm{i}\lambda(t)]\tilde{\phi}(t)$ such that $\lambda(T) - \lambda(0) = 2k\pi$ with $k = 0, \pm 1, \pm 2 \ldots$. This assumes that after projecting the nonlinear state on to the linear space, both vectors, the projected and the Floquet states in the linear space, have a phase difference $\lambda(t)$ [23]. For simplicity we take in the following $k = 0$.

Using then $\phi(t)$ and equation (B.3), we get

$$-\frac{\partial\lambda(t)}{\partial t} = \frac{1}{\mu}\langle\tilde{\phi}(t)|\tilde{\mathcal{H}}|\tilde{\phi}(t)\rangle - \langle\phi(t)|\mathrm{i}\frac{\partial}{\partial t}|\phi(t)\rangle. \tag{B.4}$$

Using equation (B.2) and integrating over a period, we find

$$0 = \frac{1}{\mu}\int_0^T \mathrm{d}t[\langle\tilde{\phi}(t)|H_0|\tilde{\phi}(t)\rangle - \langle\phi(t)|H_0|\phi(t)\rangle] - \tilde{\epsilon} + \epsilon - \frac{g}{\mu}\int_0^T \mathrm{d}t\langle\phi||\phi|^2|\phi\rangle. \tag{B.5}$$

The first term of the rhs of equation (B.5) becomes zero. Then we obtain

$$\epsilon = \tilde{\epsilon} + \frac{g}{\mu}\int_0^T \mathrm{d}t\langle\phi||\phi|^2|\phi\rangle. \tag{B.6}$$

As follows from equation (A.1), ϵ denotes the phase accumulated after a completion of one period T. To understand the physical meaning of equation (B.6), we rewrite it as a function of the real quasienergy $\tilde{\mathcal{E}}$ (see [28] for definition). It relates to our $\tilde{\epsilon}$ as $\tilde{\mathcal{E}} = \tilde{\epsilon}\mu/T$, where $-\mu\ \omega/2 < \tilde{\mathcal{E}} < \mu\ \omega/2$. Then we obtain

$$\mathcal{E} = \tilde{\mathcal{E}} + \frac{g}{T}\int_0^T \mathrm{d}t\langle\phi||\phi|^2|\phi\rangle = \tilde{\mathcal{E}} + \frac{1}{T}\int_0^T \mathrm{d}t\, g\int_0^{2\pi}\mathrm{d}x\ |\phi|^4. \tag{B.7}$$

This expression tells us that the energy of our nonlinear Floquet state is the sum of the corresponding linear and nonlinear contributions. The second term is the time average of the state energy due to the nonlinear interaction.

So far, we have considered the energy evolution of single states without perturbation. However, single states may 'coalesce' leading to bifurcations. We take the simplest case with two resonant states. We project vectors on a basis that results from the superposition of the continued original eigenstates, whose continuation lead to resonances in the nonlinear domain. That is, $\phi_j(t) = \exp[-\mathrm{i}\lambda_j(t)](a_j\tilde{\phi}_1(t) + b_j\tilde{\phi}_2(t))$ with $j = 1, 2$; where $\tilde{\phi}_1(t)$ and $\tilde{\phi}_2(t)$ are the original Floquet states.

By doing similar operations as above we get

$$\mathcal{E}_j = |a_j|^2\tilde{\mathcal{E}}_1 + |b_j|^2\tilde{\mathcal{E}}_2 + \frac{g}{T}\int_0^T \mathrm{d}t\langle\phi_j||\phi_j|^2|\phi_j\rangle, \tag{B.8}$$

where $|a_j|^2 = |\langle\tilde{\phi}_1|\phi_j\rangle|^2$ and $|b_j|^2 = 1 - |a_j|^2 = |\langle\tilde{\phi}_2|\phi_j\rangle|^2$.

References

[1] Flach S, Yevtushenko O and Zolotaryuk Y 2000 *Phys. Rev. Lett.* **84** 2358
[2] Yevtushenko O, Flach S, Zolotaryuk Y and Ovchinnikov A A 2001 *Europhys. Lett.* **54** 141
[3] Denisov S, Flach S, Ovchinnikov A A, Yevtushenko O and Zolotaryuk Y 2002 *Phys. Rev.* E **66** 041104
[4] Schanz H, Otto M-F, Ketzmerick R and Dittrich T 2001 *Phys. Rev. Lett.* **87** 070601
Schanz H, Dittrich T and Ketzmerick R 2005 *Phys. Rev.* E **71** 026228
[5] Denisov S, Morales-Molina L and Flach S 2007 *Europhys. Lett.* **79** 10007
[6] Denisov S, Morales-Molina L, Flach S and Hänggi P 2007 *Phys. Rev.* A **75** 063424
[7] Reimann P, Grifoni M and Hänggi P 1997 *Phys. Rev. Lett.* **79** 10
[8] Goychuk I, Grifoni M and Hänggi P 1998 *Phys. Rev. Lett.* **81** 649
Goychuk I, Grifoni M and Hänggi P 1998 *Phys. Rev. Lett.* **81** 2837 (erratum)
[9] Schiavoni M, Sanchez-Palencia L, Renzoni F and Grynberg G 2003 *Phys. Rev. Lett.* **90** 094101
Jones P H, Goonasekera M and Renzoni F 2004 *Phys. Rev. Lett.* **93** 073904
Gommers R, Bergamini S and Renzoni F 2005 *Phys. Rev. Lett.* **95** 073003
Gommers R, Denisov S and Renzoni F 2006 *Phys. Rev. Lett.* **96** 240604
[10] Poletti D, Benenti G, Casati G and Li B 2007 *Phys. Rev.* A **76** 023421
[11] Ritt G, Geckeler C, Salger T, Cennini G and Weitz M 2006 *Phys. Rev.* A **74** 063622
[12] Choi D and Niu Q 1999 *Phys. Rev. Lett.* **82** 2022
[13] Jona-Lasinio M *et al* 2003 *Phys. Rev. Lett.* **91** 230406
[14] Graham R and Keymer J 1991 *Phys. Rev.* A **44** 6281
[15] Thommen Q, Garreau J C and Zehnlé V 2003 *Phys. Rev. Lett.* **91** 210405
[16] Liu J, Wu B and Niu Q 2003 *Phys. Rev. Lett.* **90** 170404
[17] Flach S 2004 *Computational Studies of Discrete Breathers* ed T Dauxois, A Litvak-Hinenzon, R Mackay and A Spanoudaki (Singapore: World Scientific) pp 1–71
[18] Aubry S, Flach S, Kladko K and Olbrich E 1996 *Phys. Rev. Lett.* **76** 1607
[19] Smerzi A, Fantoni S, Giovanazzi S and Shenoy S R 1997 *Phys. Rev. Lett.* **79** 4950
[20] Eilbeck J C, Lomdahl P S and Scott A C 1985 *Physica* D **16** 318
[21] Esser B and Schanz H 1995 *Z. Phys.* B **96** 553
[22] Flach S 1996 *Physica* D **91** 223
[23] Aharonov Y and Anandan J 1987 *Phys. Rev. Lett.* **58** 1593
[24] Berry M, Keating J P and Prado S D 1998 *J. Phys. A: Math. Gen.* **31** L245
[25] Inouye S *et al* 1998 *Nature* **392** 151
[26] Mennerat-Robilliard C *et al* 1999 *Phys. Rev. Lett.* **82** 851
Sanchez-Palencia L 2004 *Phys. Rev.* E **70** 011102
[27] Johansson M and Aubry S 1997 *Nonlinearity* **10** 1151
[28] Grifoni M and Hänggi P 1998 *Phys. Rep.* **304** 229